

Engineering of Organic Photodetector for Visible Light Detection By Vacuum Thermal Deposition Method

Chairadeya,¹ Budi Sumanto,¹ Richi Estrada,² Sajal Biring,² and Shun-Wei Liu²

¹*Department of Electrical Engineering and Informatics, Vocational College,
Universitas Gadjah Mada, Jl. Yacarana Sekip Unit III, Yogyakarta, Indonesia*

²*Department of Electronic Engineering, Ming Chi University of Technology, New Taipei City, Taiwan*

Abstract: This study aimed to determine the correlation between the photoactive layer thickness of an organic photodetector device and its performance. This research engineered organic photodetectors using zinc phthalocyanine (ZnPc) and fullerene (C₆₀) as photoactive layers for detecting visible light using the vacuum thermal deposition method. Fabrication of organic photodetectors is done by varying the thickness of the photoactive layer at the same ratio. Of the four engineered organic photodetector variations, an active layer thickness of 90 nm produced the best organic photodetector performance. This photodetector has a dark current density of 1.43×10^{-6} A cm⁻², a photocurrent density of 6.19×10^{-4} A cm⁻², an external quantum efficiency (EQE) of 73.48% at a wavelength of 630 nm, with a responsivity of 0.39 A W⁻¹ at a bias voltage of -3 V.

Keywords: Organic photodetector; vacuum thermal deposition; visible light; OPD

*Corresponding author: budi.sumanto@ugm.ac.id

<http://dx.doi.org/10.12962/j24604682.v20i1.17927>
2460-4682 ©Departemen Fisika, FSAD-ITS

I. INTRODUCTION

Explorations regarding organic semiconductors are continuously being carried out due to the increasing need to replace inorganic materials with organic materials, which have more advantages, such as flexibility, transparency, and spectral selectivity capabilities in organic photodetector devices [1-3]. Organic matter refers to materials whose molecular chains are based on carbon (C) [4]. As with inorganic semiconductors, which consist of conduction and valence bands, in organic semiconductors, the conduction band is referred to as the Lowest Unoccupied Molecular Orbital (LUMO), and the valence band is referred to as the Highest Occupied Molecular Orbital (HOMO) [5].

In contrast to inorganic semiconductors, the energy levels in an organic semiconductor can be engineered more efficiently, which allows for optimizing its electronic and optical properties for applications in specific devices, for example, selecting spectra on photodetector devices [6-11]. Organic semiconductor materials consist of donors and acceptors, which are determined by the energy level of the material. The Metallo-Phthalocyanine (MPc) group, such as Zinc Phthalocyanines (ZnPc), Chloroaluminium Phthalocyanine (ClAlPc), and Copper Phthalocyanine (CuPc), is an influential for donor material. At the same time, effective acceptors come from the fullerene group, such as C₆₀ [12]. The ease of engineering and optimization of the electronic and optical properties of organic semiconductors opens up many opportunities for the use of organic semiconductors in various fields, such as

health, communications, imaging, and energy [1-3], [13-15]. Until now, organic semiconductors have been applied as materials for various electronic devices such as organic photodetectors (OPD), organic light-emitting diodes (OLED), organic photovoltaic cells, organic thin film transistors (OTFT), and others [3]. However, studies on organic semiconductors, especially organic photodetectors, have not been carried out in Indonesia. Therefore, in this study, research was carried out on organic photodetectors by fabricating organic photodetectors that are sensitive to visible light, using the vacuum thermal deposition method to determine the correlation between the thickness of the active layer of organic photodetectors and their performance. In addition, organic photodetectors will be engineered in such a way as to produce organic photodetectors with low dark current density values but still maintain external quantum efficiency (EQE) and responsivity values.

In a previous study, an organic photodetector was made using the vacuum thermal deposition method, with a ZnPc: C₆₀ material ratio of 1:1 with a 40 nm thickness deposited by bulk heterojunction. From the study, it was found that the use of Zinc Phthalocyanine (ZnPc) and fullerene (C₆₀) as active materials has good performance in the detection of visible light [16]. In this study, organic photodetectors were made by varying the thickness of the photoactive layer, using ZnPc: C₆₀ material with a ratio of 1:3. The increased ratio of C₆₀ used in this study is based on research by Goldberg et al, that C₆₀ material has a significant value of charge mobility so that the dominance of C₆₀ material in the active layer is expected to increase the EQE value of a photodetector [17].

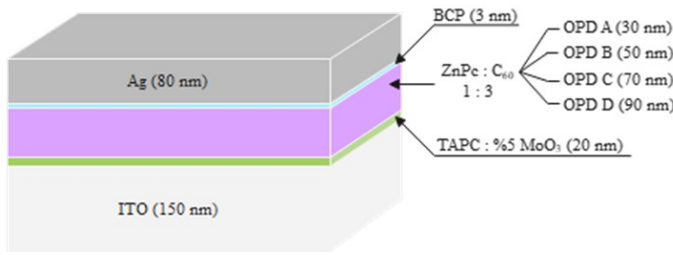


FIG. 1: Organic Photodetector Structure.

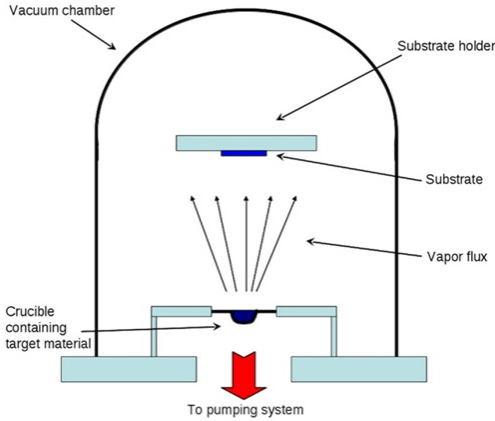


FIG. 2: Schematic of Vacuum Thermal Deposition Method [18].

II. METHODOLOGY

A. Fabrication of Organic Photodetector Devices

Fig. 1 shows the structure of the engineered device. In this study, the OPD device was fabricated using the vacuum thermal deposition method in a vacuum chamber with a pressure $<10^{-6}$ torr in an active area of 4 mm^2 [12, 18]. The Schematic of this method can be seen in Fig. 2. At first, 1,1-Bis[(di-4-alkylamino)phenyl]cyclohexane (TAPC): 5% molybdenum (IV) oxide (MoO_3) (with a thickness of 20 nm) was deposited as an electron-blocking layer, on an Indium Tin Oxide coated glass substrate ($29 \times 19 \text{ mm}$). In the second step, the ZnPc: C_{60} photoactive layer was deposited in a ratio of 1:3, with four variations in the thickness of the active layer. The photoactive layer is deposited by bulk heterojunction to improve charge separation efficiency. In the third step, a thin layer of BCP (with a thickness of 3 nm) was deposited as the hole-blocking layer. At last, silver (Ag) (with a thickness of 80 nm) was deposited as the cathode. The thickness of each layer deposited in the film is precisely monitored and controlled in real-time by a Quartz Crystal Microbalance (QCM) sensor within the vacuum chamber. By meticulously tracking the crystal's resonant frequency, the QCM provides invaluable real-time feedback on film thickness, ensuring optimal deposition parameters and layer-by-layer precision. To maintain performance, the OPD device was encapsulated in a glove box under a controlled atmosphere ($\text{O}_2 < 0.1 \text{ ppm}$;

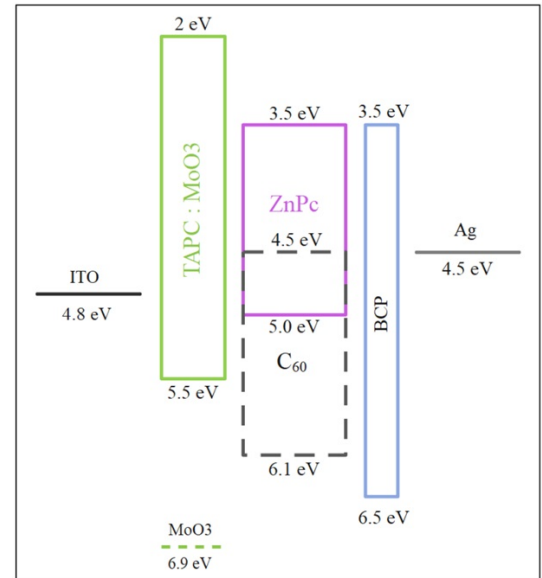


FIG. 3: Energy Level Diagram of The OPD Device.

TABLE I: The result of OPD Device Characterization.

OPD	Dark Current (A/cm^{-2})	Photo Current (A/cm^{-2})	EQE (%)	Responsivitas (A/W)
A	7.17E-04	2.14E-04	31.93	0.17
B	2.09E-05	3.39E-04	65.21	0.34
C	3.49E-06	5.09E-04	71.34	0.38
D	1.43E-06	6.19E-04	73.48	0.39

$\text{H}_2\text{O} < 0.1 \text{ ppm}$) using an opaque glass substrate ($27 \times 19 \text{ mm}^2$), which was then bonded with UV-curable epoxy resin and dried under UV light [12].

B. Characterization of Organic Photodetector Devices

The characterization of the OPD device in the first stage was carried out using a Keithley 2636A Sourcemeater in the dark to obtain dark current density characteristics. Measurements were done under voltage sweep-control from 3 to -3 V, with a voltage step of 0.01 V. Then Keithley 2401 SourceMeter was used to obtain the photocurrent density characteristics, under voltage sweep-control from 3 to -3 V, with a voltage step of 0.01 V, while illuminated with one sun illumination from the solar simulator (Newport 91160A) with intensity was set to 100 mW cm^{-2} . Then the spectra of external quantum efficiency (EQE) and responsivity of OPD were measured using the QE-R system (Enlitech, Taiwan) in the visible light wavelength range (300-800 nm), with a wavelength step of 5 nm. The results of each measurement are then plotted using the Origin software to obtain a graph of each measured characteristic.

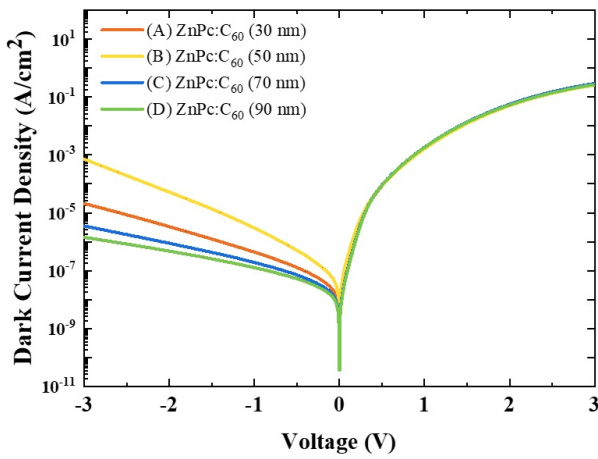


FIG. 4: The Dark Current Density Characteristic of OPD Device.

III. RESULT AND DISCUSSION

The results of the OPD characterization are shown in Table I, where the photodetector was fabricated with four different thickness variations, namely OPD A (30 nm), OPD B (50 nm), OPD C (70 nm), and OPD D (90 nm). In a study by Estrada *et al.*, it was stated that the performance of an OPD device depends on the low value of the dark current density. In this study, the dark current density (J_d) of OPD A, B, C, and D reached 717, 20.9, 3.49, and $1.43 \mu\text{A cm}^{-2}$ values. The lower the dark current density value of a photodetector, the better the performance of other characteristics [19]. The performance of the organic photodetector itself can be related to the energy level and thickness of each layer of its architecture. In Fig. 3, it can be seen the energy level of each material composing the engineered organic photodetector layer structure.

The results of the characterization of dark current density can be seen in Fig. 4. The graph shows that OPD D has the best dark current density value, namely $1.43 \times 10^{-6} \text{ A/cm}^2$ at -3 V voltage bias. The low value of dark current density is obtained from the engineering of the thickness of the photoactive layer of the OPD and the use of blocking layers. If seen from the measurement results, the OPD with the lowest dark current density value is OPD D with the highest active layer thickness, which is 90 nm. Where in the graph, it can be seen that the thicker the active layer, the lower the resulting dark current density value. The thicker the photoactive layer, the more difficult it is for the charge to move from the photoactive layer to the electrode layer without any interaction between light and the photoactive layer [5]. However, if the active layer is too thick or, in other words, not optimal, then the level of light absorption by the OPD will decrease so that the EQE value and responsiveness will also decrease. Then using BCP material as a hole-blocking layer also suppresses the dark current density value. The low energy level of HOMO from BCP prevents holes from penetrating from the active layer toward the cathode. So that there is no current leakage in dark conditions and a low dark current density

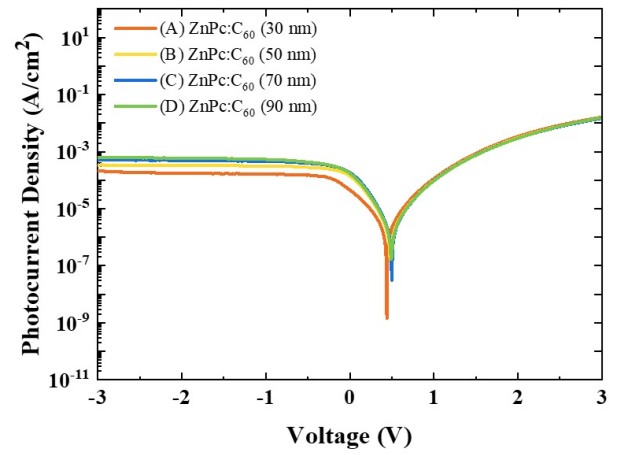


FIG. 5: The Photocurrent Density Characteristic of OPD Device.

value is produced.

Then the results of the characterization of the photocurrent density can be seen in Fig. 5. The graph shows that OPD D, with a thickness of 90 nm, has the best photocurrent density value, which is $6.19 \times 10^{-4} \text{ A/cm}^2$ at a bias voltage of -3 V. Several factors, such as the thickness of the active layer, the charge carrier mobility of the material, the efficiency of absorption of light from the photodetector, the energy level of the device structure, and the light intensity at the time of measurement influence the difference in values for each of these variations.

In the graph, it can be seen that the thicker the active layer, the higher the resulting photocurrent density value. Then from the material side, theoretically, the acceptor (C_{60}) has a significant value of charge mobility, which can simultaneously increase the efficiency of absorbing light from an OPD device [17]. The high photocurrent value of the OPD device is also associated with good device structure. Fig. 3 shows that the blocking layer used has a higher HOMO energy than the active layer on the EBL side and has the same LUMO energy as the active layer on the HBL side. This then facilitates the transfer of holes to the anode and electrons to the cathode so that the process of transferring electrons and holes becomes more efficient and increases the resulting photocurrent value.

Furthermore, the results of the characterization of the EQE value and the responsiveness of the OPD measured at a bias voltage of -3 V can be seen in Fig. 6. In the graph, it can be seen that there are two peaks of EQE and responsivity at a wavelength of 350 nm and 630-690 nm. The first peak (UV light waves) results from light absorption by the C_{60} material, and the second peak (visible light waves) results from light absorption by the ZnPc material. However, in this study, organic photodetectors were engineered in such a way as to produce visible light-sensitive organic photodetectors. Therefore, engineering was carried out on the ratio and thickness of the active layer, as well as the addition of an appropriate blocking layer. Thus the OPD is obtained that has a high EQE value for two light waves but only has a high responsivity for

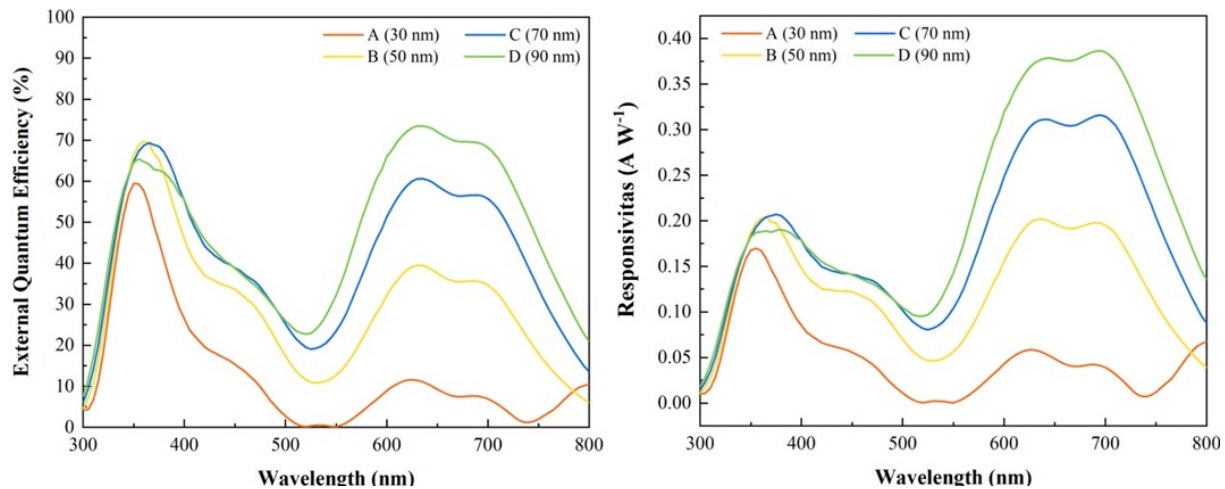


FIG. 6: The External Quantum Efficiency (EQE) and Responsivity Characteristic of OPD Device.

visible light, so the engineered OPD will be more sensitive to visible light waves compared to UV waves.

Apart from being affected by the structure of the device, the EQE value and responsivity can also be affected by the applied bias voltage during measurement. The application of bias voltage can affect photon absorption, charge transport, and charge extraction efficiency, affecting the value of EQE and responsiveness [20]. The bias voltage can change the electronic energy distribution in the active layer, which then affects the photon-electron interactions. This change can shift the absorption wavelength or modulate the absorption efficiency of a photon at a particular wavelength. In other words, photon absorption can be increased by optimizing the bias voltage.

IV. CONCLUSION

This study obtained organic photodetectors with the best performance with a photoactive layer thickness of 90 nm. Where in the characterization carried out obtained a dark current density value of 1.43×10^{-6} A/cm², a photocurrent den-

sity value of 6.19×10^{-4} A/cm², and an EQE value of 73.48% at a wavelength of 630 nm with a responsivity of 0.39 A/W at a bias voltage of -3 V. This shows that the fabricated photodetector is sensitive to visible light, and has a low dark current density value while maintaining the EQE and responsivity value. The characterization results indicate that the active layer thickness affects the performance of an OPD, where the optimal active layer thickness will simultaneously optimize the performance of the OPD device. So it is critical to find the optimal active layer thickness to achieve the best performance from an organic photodetector.

Acknowledgments

The Organic Electronic Research Center, Ming Chi University of Technology, New Taipei City, Taiwan, 2023, and Indonesian International Student Mobility Awards Edisi Vokasi (IISMAeVo) 2022 by The Ministry of Education, Culture, Research, and Technology of Republic Indonesia, supported this research.

- [1] T. Shan, *et al.*, "Organic photodiodes: device engineering and applications", vol. 15, no. 1. Higher Education Press, 2022. doi: 10.1007/s12200-022-00049-w.
- [2] G. Simone, *et al.*, "Organic Photodetectors and their Application in Large Area and Flexible Image Sensors: The Role of Dark Current", *Adv. Funct. Mater.*, vol. 30, no. 20, 2020, doi: 10.1002/adfm.201904205.
- [3] H. Ren, *et al.*, "Recent Progress in Organic Photodetectors and their Applications", *Adv. Sci.*, vol. 8, no. 1, pp. 123, 2021, doi: 10.1002/advs.202002418.
- [4] S. Ahmad, "Organic semiconductors for device applications: Current trends and future prospects", *J. Polym. Eng.*, vol. 34, no. 4, pp. 279338, 2014, doi: 10.1515/polyeng-2013-0267.
- [5] Y. Li, H. Chen, and J. Zhang, "Carrier blocking layer materials

and application in organic photodetectors", *Nanomaterials*, vol. 11, no. 6, 2021, doi: 10.3390/nano11061404.

- [6] D. Nath, *et al.*, "Zero bias high responsive visible organic photodetector based on pentacene and C60", *Opt. Laser Technol.*, vol. 131, no. April, p. 106393, 2020, doi: 10.1016/j.optlastec.2020.106393.
- [7] J. B. Park, *et al.*, "Visible-Light-Responsive High-Detectivity Organic Photodetectors with a 1 m Thick Active Layer", *ACS Appl. Mater. Interfaces*, vol. 10, no. 44, pp. 3829438301, 2018, doi: 10.1021/acsami.8b13550.
- [8] C. H. Swartz and C. B. Winstead, "Fast response organic photodetectors with a thick photoconversion region and fullerene transport layer", *Mater. Sci. Semicond. Process.*, vol. 91, no. October 2018, pp. 2226, 2019, doi:

- 10.1016/j.mssp.2018.11.001.
- [9] L. Lv, *et al.*, "Significant enhancement of responsivity of organic photodetectors upon molecular engineering", *J. Mater. Chem. C*, vol. 7, no. 19, pp. 57395747, 2019, doi: 10.1039/c9tc00576e.
- [10] L. Li, *et al.*, "Intelligent metasurfaces: control, communication and computing", *eLight*, vol. 2, no. 1, 2022, doi: 10.1186/s43593-022-00013-3.
- [11] J. Pan, *et al.*, "Photodetectors based on small-molecule organic semiconductor crystals", *Chinese Phys. B*, vol. 28, no. 3, 2019, doi: 10.1088/1674-1056/28/3/038102.
- [12] R. Estrada, *et al.*, "Developing efficient small molecule-based organic photo-couplers by optimizing the cathode interfacial layer in the photodetector", *J. Mater. Chem. C*, pp. 53785387, 2023, doi: 10.1039/d3tc00188a.
- [13] Y. Khan, *et al.*, "Organic multi-channel optoelectronic sensors for wearable health monitoring", *IEEE Access*, vol. 7, pp. 128114128124, 2019, doi: 10.1109/ACCESS.2019.2939798.
- [14] L.E.M. Matheus, *et al.*, "Visible Light Communication: Concepts, Applications and Challenges", *IEEE Commun. Surv. Tutorials*, vol. 21, no. 4, pp. 32043237, 2019, doi: 10.1109/COMST.2019.2913348.
- [15] C. Vega-Colado, *et al.*, "An all-organic flexible visible light communication system", *Sensors (Switzerland)*, vol. 18, no. 9, pp. 112, 2018, doi: 10.3390/s18093045.
- [16] T. Otto, *et al.*, "Highly sensitive wide range organic photodiode based on zinc phthalocyanine:C 60", vol. 5, no. 2016, pp. 15, 2019, doi: 10.1002/pssa.201532856.
- [17] A. Goldberg, *et al.*, "Estimation of electron and hole mobility of 50 homogeneous fullerene amorphous structures (C60, C58B2, C58N2 and C58NB) using a percolation corrected Marcus theory model", *Org. Electron.*, vol. 78, p. 105571, 2020, doi: 10.1016/j.orgel.2019.105571.
- [18] R.J. Martn-Palma and A. Lakhtakia, "Vapor-Deposition Techniques", in *Engineered Biomimicry*, Pennsylvania: Elsevier Inc., 2013, pp. 383398. doi: 10.1016/B978-0-12-415995-2.00015-5.
- [19] R. Estrada, *et al.*, "Developing efficient small molecule-based organic photo-couplers by optimizing the cathode interfacial layer in the photodetector", *J. Mater. Chem. C*, 2023, doi: 10.1039/d3tc00188a.
- [20] Z. Zhao, *et al.*, "Recent Progress on Broadband Organic Photodetectors and their Applications", *Laser Photonics Rev.*, vol. 14, no. 11, pp. 124, 2020, doi: 10.1002/lpor.202000262.